Effect of the Wall on the Velocity Autocorrelation Function and Long-Time Tail of Brownian Motion†

B. U. Felderhof*

Institut für Theoretische Physik A, RWTH Aachen, Templergraben 55, 52056 Aachen, Germany

Received: March 15, 2005; In Final Form: April 22, 2005

Brownian motion of a particle situated near a wall bounding the fluid in which it is immersed is affected by the wall. Specifically, it is assumed that an incompressible viscous fluid fills a half-space bounded by a plane wall and that the fluid flow satisfies stick boundary conditions at the wall. The fluctuation−dissipation theorem shows that the velocity autocorrelation function of the Brownian particle can be calculated from the frequency-dependent admittance valid locally. It is shown that the $t^{-3/2}$ long-time tail of the velocity relaxation function, valid in bulk fluid, is obliterated and replaced by a $t^{-5/2}$ long-time tail of positive amplitude for motions parallel to the wall and by a $t^{-5/2}$ long-time tail of negative amplitude for motions perpendicular to the wall. The latter finding is at variance with an earlier calculation by Gotoh and Kaneda.

1. Introduction

It is well-known that the velocity autocorrelation function of a Brownian particle immersed in bulk fluid decays at long times with a $t^{-3/2}$ tail with an amplitude independent of size or mass of the particle. The amplitude depends only on the temperature and kinematic viscosity of the fluid in which it is immersed. The nature of the long-time tail is determined by the long-time diffusion of momentum in the viscous fluid and thus may be affected by the presence of a wall. By the fluctuation−dissipation theorem, the correlation function may be calculated from the frequency-dependent admittance.[1−5] Thus, the calculation reduces to a study in linear hydrodynamics and can be based on the linearized Navier−Stokes equations.

The influence of a wall on the steady-state friction coefficient was calculated long ago by Lorentz.[6] His calculation was extended to nonzero frequency by Wakiya[7] for motion parallel to the wall. Motion perpendicular to the wall was studied by Gotoh and Kaneda.[8] These authors showed that the $t^{-3/2}$ long-time tail of bulk Brownian motion is obliterated by the wall. They derived a $t^{-5/2}$ long-time tail with positive amplitude for motions parallel to the wall and a $t^{-7/2}$ long-time tail with positive amplitude for motions perpendicular to the wall. We show in the following that the latter result is erroneous. Actually for motion perpendicular to the wall, the velocity correlation function has a $t^{-5/2}$ long-time tail with negative amplitude.

In the following, we calculate the frequency-dependent admittance of a particle near a wall in point approximation, i.e., to first order in the ratio a/h, where a is the particle radius and h is the distance to the wall. Gotoh and Kaneda[8] did not calculate the effect of particle mass on the admittance, and thus did not apply the fluctuation−dissipation theorem correctly. Also they restricted attention to the long-time behavior. Our calculation yields the complete time-dependence of the velocity autocorrelation function. The long-time results of Gotoh and Kaneda have been confirmed in computer simulation by Pagonabarraga et al.,[9] but in their work the fully asymptotic regime was not reached, so that they did not see the change of sign of the correlation function for motions perpendicular to the wall.

2. Linear Hydrodynamics

We consider a spherical particle of radius a and mass m_p, immersed in a viscous incompressible fluid of shear viscosity η and mass density ρ. The sphere and the fluid are confined to volume Ω with boundary $\Sigma(\Omega)$. The fluid is assumed to satisfy stick boundary conditions at $\Sigma(\Omega)$ and at the surface of the sphere. We shall investigate the effect of a time-dependent force $\boldsymbol{E}(t)$ acting at the center of the particle on the motion of both fluid and particle. The force will be assumed to be small, so that we can use linearized equations of motion. The center of the particle performs small motions about the rest position $\boldsymbol{r}_0$.

For small-amplitude motion the flow velocity $\boldsymbol{v}(\boldsymbol{r}, t)$ and the pressure $p(\boldsymbol{r}, t)$ are governed by the linearized Navier−Stokes equations

$$\rho\frac{\partial \boldsymbol{v}}{\partial t} = \eta\nabla^2\boldsymbol{v} - \nabla p$$
$$\nabla\cdot \boldsymbol{v} = 0 \tag{2.1}$$

The pressure $p(\boldsymbol{r}, t)$ is determined by the condition of incompressibility. After Fourier analysis in time, we find that the equations for the Fourier components with time-factor $\exp(-i\omega t)$ are

$$\eta(\nabla^2\boldsymbol{v}_\omega - \alpha^2\boldsymbol{v}_\omega) - \nabla p_\omega = 0, \quad \nabla\cdot \boldsymbol{v}_\omega = 0 \tag{2.2}$$

where we have used the abbreviation

$$\alpha = (-i\omega\rho/\eta)^{1/2}, \quad \mathscr{R}\alpha > 0 \tag{2.3}$$

The equation of motion for the particle may be written in Fourier language as

$$-i\omega(m_p - m_f)\boldsymbol{U}_\omega = -\mathscr{F}_\omega + \boldsymbol{E}_\omega \tag{2.4}$$

where $m_f = 4\pi a^3\rho/3$ is the mass of fluid displaced by the sphere and $\mathscr{F}_\omega$ is the total induced force exerted by the particle on the

† Part of the special issue "Irwin Oppenheim Festschrift".

* To whom correspondence should be addressed. E-mail: ufelder@physik.rwth-aachen.de.

10.1021/jp051335b CCC: $30.25
Published on Web 05/27/2005

fluid.[10] In the presence of an incident flow ($v'_\omega(\boldsymbol{r})$, $p'_\omega(\boldsymbol{r})$), satisfying the homogeneous equations (2.2), one finds for the induced force[11−13]

$$\mathcal{F}_\omega = \left[\zeta(\omega) - \frac{3}{2}i\omega m_f\right](\boldsymbol{U}_\omega - \overline{\boldsymbol{v}'_\omega}^S) - \lambda(\omega)(\overline{\boldsymbol{v}'_\omega}^V - \overline{\boldsymbol{v}'_\omega}^S) \quad (2.5)$$

where $\overline{\boldsymbol{v}'_\omega}^S$ denotes an average over the sphere surface and $\overline{\boldsymbol{v}'_\omega}^V$ an average over the sphere volume. The frequency-dependent friction coefficient is given by

$$\zeta(\omega) = 6\pi\eta a(1 + \alpha a) \quad (2.6)$$

The coefficient $\lambda(\omega)$ in eq 2.5 takes account of the spatial inhomogeneity of the acting flow. In the point−particle limit, the second term in eq 2.5 can be neglected. The acting flow can be expressed as

$$\boldsymbol{v}'_\omega(\boldsymbol{r}) = \boldsymbol{v}_\omega(\boldsymbol{r}) - \boldsymbol{v}_{0\omega}(\boldsymbol{r}) \quad (2.7)$$

where $\boldsymbol{v}_{0\omega}(\boldsymbol{r})$ is the solution for infinite space and $\boldsymbol{v}_\omega(\boldsymbol{r})$ is the solution in the presence of the bounding surface. In the point−particle limit, both flows are given by the appropriate Green function

$$\boldsymbol{v}_\omega(\boldsymbol{r}) = \mathbf{G}(\boldsymbol{r},\boldsymbol{r}_0)\cdot\boldsymbol{E}_\omega,\ \boldsymbol{v}_{0\omega}(\boldsymbol{r}) = \mathbf{G}_0(\boldsymbol{r} - \boldsymbol{r}_0)\cdot\boldsymbol{E}_\omega \quad (2.8)$$

We do not indicate the dependence of the Green functions on frequency ω explicitly. The Green function for infinite space is translationally invariant, and given explicitly by[10]

$$\mathbf{G}_0(\boldsymbol{r}) = \frac{1}{4\pi\eta}\left(\frac{e^{-\alpha r}}{r}\mathbf{1} + \alpha^{-2}\nabla\nabla\frac{1 - e^{-\alpha r}}{r}\right) \quad (2.9)$$

We define the reaction field tensor $\mathbf{F}(\boldsymbol{r}_0,\omega)$ by

$$\mathbf{F}(\boldsymbol{r}_0,\omega) = \lim_{\boldsymbol{r}\to\boldsymbol{r}_0}(\mathbf{G}(\boldsymbol{r},\boldsymbol{r}_0) - \mathbf{G}_0(\boldsymbol{r} - \boldsymbol{r}_0)) \quad (2.10)$$

In the point-particle limit the induced force becomes

$$\mathcal{F}_\omega = \left[\zeta(\omega) - \frac{3}{2}i\omega m_f\right](\boldsymbol{U}_\omega - \mathbf{F}(\boldsymbol{r}_0,\omega)\cdot\boldsymbol{E}_\omega) \quad (2.11)$$

Substituting this into the equation of motion (2.4) and solving for the velocity $\boldsymbol{U}_\omega$, we obtain

$$\boldsymbol{U}_\omega = \mathcal{Y}(\boldsymbol{r}_0,\omega)\cdot\boldsymbol{E}_\omega \quad (2.12)$$

with admittance tensor given by[13,14]

$$\mathcal{Y}(\boldsymbol{r}_0,\omega) = \mathcal{Y}_0(\omega)\left[\mathbf{1} + 6\pi\eta a\left(1 + \alpha a + \frac{1}{3}\alpha^2 a^2\right)\boldsymbol{F}(\boldsymbol{r}_0,\omega)\right] \quad (2.13)$$

where $\mathcal{Y}_0(\omega)$ is the scalar admittance for infinite space

$$\mathcal{Y}_0(\omega) = \left[-i\omega m_p + 6\pi\eta a\left(1 + \alpha a + \frac{1}{9}\alpha^2 a^2\right)\right]^{-1} = \left[-i\omega\left(m_p + \frac{1}{2}m_f\right) + \zeta(\omega)\right]^{-1} \quad (2.14)$$

Here the term $\frac{1}{2}m_f$ is the added mass. The reaction field tensor $\mathbf{F}(\boldsymbol{r}_0,\omega)$ can be evaluated only for simple geometry. In the following we consider a half-space bounded by a plane wall.

3. Green Functions and Reaction Field Tensor

We consider the half-space $z > 0$ with a wall at $z = 0$ where the fluid satisfies stick boundary conditions. To calculate the Green function $\mathbf{G}(\boldsymbol{r},\boldsymbol{r}_0)$, we employ the method developed by Jones[15] for the case $\omega = 0$.

By translational symmetry we expect $\mathbf{G}(\boldsymbol{r},\boldsymbol{r}_0)$ to depend only on the differences $x - x_0$ and $y - y_0$, so that we can introduce a two-dimensional Fourier transform in the xy plane. With two-dimensional position vectors $\boldsymbol{s} = (x, y)$ and $\boldsymbol{s}_0 = (x_0, y_0)$, we express $\mathbf{G}(\boldsymbol{r},\boldsymbol{r}_0)$ as $\mathbf{G}(\boldsymbol{s} - \boldsymbol{s}_0, z, z_0)$ and transform it as

$$\mathbf{G}(\boldsymbol{s} - \boldsymbol{s}_0, z, z_0) = \int d\boldsymbol{q}\, e^{i\boldsymbol{q}\cdot(\boldsymbol{s}-\boldsymbol{s}_0)}\hat{\mathbf{G}}(\boldsymbol{q}, z, z_0) \quad (3.1)$$

The undisturbed particle position is taken as $\boldsymbol{r}_0 = (0, 0, h)$. To find the elements $G_{\alpha x}(\boldsymbol{r},\boldsymbol{r}_0)$ of the Green tensor we must solve the ordinary differential equations

$$\eta\left(\frac{d^2}{dz^2} - (q^2 + \alpha^2)\right)\hat{v}_x(\boldsymbol{q}, z) - iq_x\hat{p}(\boldsymbol{q}, z) = \frac{-1}{4\pi^2}\delta(z - h)$$

$$\eta\left(\frac{d^2}{dz^2} - (q^2 + \alpha^2)\right)\hat{v}_y(\boldsymbol{q}, z) - iq_y\hat{p}(\boldsymbol{q}, z) = 0$$

$$\eta\left(\frac{d^2}{dz^2} - (q^2 + \alpha^2)\right)\hat{v}_z(\boldsymbol{q}, z) - \frac{d\hat{p}(\boldsymbol{q}, z)}{dz} = 0 \quad (3.2)$$

with the incompressibility condition

$$iq_x\hat{v}_x(\boldsymbol{q}, z) + iq_y\hat{v}_y(\boldsymbol{q}, z) + \frac{d\hat{v}_z(\boldsymbol{q}, z)}{dz} = 0 \quad (3.3)$$

Similar sets of equations are to be solved for the elements $G_{\alpha y}(\boldsymbol{r},\boldsymbol{r}_0)$ and $G_{\alpha z}(\boldsymbol{r},\boldsymbol{r}_0)$. For our purpose it suffices to consider the elements $\hat{G}_{xx}(\boldsymbol{q}, z, h)$ and $\hat{G}_{zz}(\boldsymbol{q}, z, h)$. The explicit expression for the element $\hat{G}_{xx}(\boldsymbol{q}, z, h)$ is

$$\hat{G}_{xx}(\boldsymbol{q}, z, h) = \frac{1}{8\pi^2\eta q\alpha^2}\left[\frac{q}{q - s}(q(q + s)\, e^{-qh-qz} - q(q - s)\, e^{-q|z-h|} + s(q - s)\, e^{-s|z-h|} + s(q + s)\, e^{-sh-sz} - 2qs\, e^{-qh-sz} - 2qs\, e^{-sh-qz}) + \frac{q_y^2(q + s)}{\alpha^2 s}(s(q + s)\, e^{-qh-qz} - s(q - s)\, e^{-q|z-h|} + q(q - s)\, e^{-s|z-h|} - (q^2 - qs - 2s^2)\, e^{-sh-sz} - 2s^2\, e^{-qh-sz} - 2s^2\, e^{-sh-qz})\right] \quad (3.4)$$

with the abbreviation

$$s = \sqrt{q^2 + \alpha^2} \quad (3.5)$$

Similarly the expression for the element $\hat{G}_{zz}(\boldsymbol{q}, z, h)$ is

$$\hat{G}_{zz}(\boldsymbol{q}, z, h) = \frac{q}{8\pi^2\eta s(q - s)\alpha^2}[s(q + s)\, e^{-qh-qz} + s(q - s)\, e^{-q|z-h|} - q(q - s)\, e^{-s|z-h|} + q(q + s)\, e^{-sh-sz} - 2qs\, e^{-qh-sz} - 2qs\, e^{-sh-qz}] \quad (3.6)$$

The corresponding expressions for the infinite space Green functions are

$$\hat{G}_{0xx}(\boldsymbol{q}, z, h) = \frac{1}{8\pi^2\eta qs\alpha^2}[-q_x^2 s\, e^{-q|z-h|} + q(s^2 - q_y^2)\, e^{-s|z-h|}]$$

$$\hat{G}_{0zz}(\boldsymbol{q}, z, h) = \frac{q}{8\pi^2\eta s\alpha^2}[s e^{-q|z-h|} - q e^{-s|z-h|}] \quad (3.7)$$

The elements of the reaction field tensor defined in eq 2.10 can now be evaluated from an integral over two-dimensional wavevectors $\boldsymbol{q}$

$$F_{\alpha\beta}(\boldsymbol{r}_0,\omega) = \int [\hat{G}_{\alpha\beta}(\boldsymbol{q}, h, h) - \hat{G}_{0\alpha\beta}(\boldsymbol{q}, h, h)]\, \mathrm{d}\boldsymbol{q} \quad (3.8)$$

The integrals can be evaluated explicitly. For the xx-element we find in terms of the variable $v = \alpha h$

$$F_{xx}(\boldsymbol{r}_0,\omega) = \frac{-1}{192\pi\eta h v^4}[36 + 27v + 6v^2 + 6(6 + 12v + 11v^2 + 6v^3 + 4v^4)\,\mathrm{e}^{-2v} - (144 + 144v + 72v^2 + 24v^3 - 6v^4 + 2v^5 - v^6 + v^7)\,\mathrm{e}^{-v} + v^8 E_1(v) + 12v^3(2vK_2(2v) + 3K_3(2v)) + 6\pi v^3(2vY_2(2v) - 3Y_3(2v) - 3\boldsymbol{H}_{-3}(2v) - 2v\boldsymbol{H}_{-2}(2v))] \quad (3.9)$$

with Bessel functions $Y_n(2v)$, modified Bessel functions $K_n(2v)$, the exponential integral $E_1(v)$, and Struve functions $\boldsymbol{H}_n(2v)$. For the zz element we find

$$F_{zz}(\boldsymbol{r}_0,\omega) = \frac{-1}{96\pi\eta h v^2}[6(6 + v^2 + 8v^3) + 6(6 + 12v + 9v^2 + 2v^3)\,\mathrm{e}^{-2v} - (144 + 144v + 48v^2 - 6v^4 + 10v^5 + v^6 - v^7)\,\mathrm{e}^{-v} + v^6(12 - v^2)E_1(v) + 12v^2K_0(2v) + 6v(2 + v^2)K_1(2v) + 6\pi(2v(3 - v^2)(Y_0(2v) - \boldsymbol{H}_0(2v)) - (6 - 5v^2)(Y_1(2v) - \boldsymbol{H}_1(2v)))] \quad (3.10)$$

The elements $F_{xy}(\boldsymbol{r}_0,\omega)$ and $F_{yx}(\boldsymbol{r}_0,\omega)$ vanish by axial symmetry, and it can be checked that the elements $F_{xz}(\boldsymbol{r}_0,\omega)$, $F_{zx}(\boldsymbol{r}_0,\omega)$, $F_{yz}(\boldsymbol{r}_0,\omega)$, and $F_{zy}(\boldsymbol{r}_0,\omega)$ also vanish. The element $F_{yy}(\boldsymbol{r}_0,\omega)$ equals $F_{xx}(\boldsymbol{r}_0,\omega)$.

At this point we make contact with earlier work on the zero-frequency case. The function $F_{xx}(\boldsymbol{r}_0)$ in eq 3.9 has the low-frequency expansion

$$F_{xx}(\boldsymbol{r}_0,\omega) = \frac{1}{6\pi\eta h}\left(-\frac{9}{16} + v - \frac{9}{8}v^2 + v^3 + \frac{3}{16}v^4 \log v + O(v^4)\right) \quad (3.11)$$

whereas the function $F_{zz}(\boldsymbol{r}_0,\omega)$ in eq 3.10 has the low-frequency expansion

$$F_{zz}(\boldsymbol{r}_0,\omega) = \frac{1}{6\pi\eta h}\left(-\frac{9}{8} + v - \frac{3}{8}v^2 + \frac{19}{192}v^4 - \frac{1}{10}v^5 + O(v^6)\right) \quad (3.12)$$

Substituting this into eq 2.13 we find for the zero-frequency mobility parallel to the wall

$$\mu_{xx}(\boldsymbol{r}_0) = \frac{1}{6\pi\eta a}\left(1 - \frac{9a}{16h}\right) \quad (3.13)$$

and for the zero-frequency mobility perpendicular to the wall

$$\mu_{zz}(\boldsymbol{r}_0) = \frac{1}{6\pi\eta a}\left(1 - \frac{9a}{8h}\right) \quad (3.14)$$

These results were derived by Lorentz by the method of images.[6] In an alternative calculation, one can obtain these results by first taking the limit $\alpha \to 0$ in the expressions for the Green functions.

4. Velocity Autocorrelation Functions

In the preceding section, we have found explicit expressions for the elements $\mathscr{Y}_{xx}(\omega)$ and $\mathscr{Y}_{zz}(\omega)$ of the admittance tensor giving the linear response to a frequency-dependent force applied to the particle. In principle, this allows one to calculate by Fourier transform the functions describing velocity relaxation after a sudden applied impulse. In the theory of Brownian motion the velocity correlation functions of a Brownian particle are defined by

$$C_{\alpha\beta}(t) = \langle U_\alpha(t)U_\beta(0)\rangle \quad (4.1)$$

where the angle brackets denote the equilibrium ensemble average. We define the one-sided Fourier transform as

$$\hat{C}_{\alpha\beta}(\omega) = \int_0^\infty \mathrm{e}^{\mathrm{i}\omega t} C_{\alpha\beta}(t)\, \mathrm{d}t \quad (4.2)$$

According to the fluctuation–dissipation theorem the Fourier transform is given by

$$\hat{C}_{\alpha\beta}(\omega) = k_B T \mathscr{Y}_{\alpha\beta}(\omega) \quad (4.3)$$

From eq 3.8, one finds that for large positive v the reaction field factors $F_{xx}(\boldsymbol{r}_0,\omega)$ and $F_{zz}(\boldsymbol{r}_0,\omega)$ behave as

$$F_{xx}(\boldsymbol{r}_0,\omega) \approx \frac{-3}{32\pi\eta h v^2}, \quad F_{zz}(\boldsymbol{r}_0,\omega) \approx \frac{-3}{16\pi\eta h v^2} \quad (4.4)$$

Hence eq 2.13 yields for the initial value of the correlation functions

$$C_{xx}(0+) = \frac{k_B T}{m^*}\left(1 - \frac{a^3}{16h^3}\right), \quad C_{zz}(0+) = \frac{k_B T}{m^*}\left(1 - \frac{a^3}{8h^3}\right) \quad (4.5)$$

where $m^* = m_p + 1/2\, m_f$ is the effective mass. The equipartition theorem applied to eq 4.1 would yield the prefactor $k_B T/m_p$ instead. The difference is due to the assumption of fluid incompressibility, as explained by Zwanzig and Bixon.[1] The rapid initial decrease on the time scale $\tau_s = a/c$, where c is the velocity of sound, is ignored.

We write the correlation function $C_{xx}(t)$ in the form[16]

$$C_{xx}(t) = \frac{k_B T}{m^*}\left(1 - \frac{a^3}{16h^3}\right)\gamma_{xx}(t/\tau_{Mx}) \quad (4.6)$$

with a relaxation function $\gamma_{xx}(\tau)$ that decays to zero starting from the initial value $\gamma(0+) = 1$, and with a mean relaxation time τ_{Mx} defined by

$$\tau_{Mx} = \frac{1}{C_{xx}(0+)}\int_0^\infty C_{xx}(t)\, dt \quad (4.7)$$

Similar definitions are made for $C_{zz}(t)$. From eqs 3.13 and 3.14, we find

$$\tau_{Mx} = \frac{m^*}{6\pi\eta a}\frac{1 - 9a/16h}{1 - a^3/16h^3}, \quad \tau_{Mz} = \frac{m^*}{6\pi\eta a}\frac{1 - 9a/8h}{1 - a^3/8h^3} \quad (4.8)$$

The Laplace transform of the relaxation functions is defined as

$$\Gamma_x(z) = \int_0^\infty \mathrm{e}^{-z\tau}\gamma_{xx}(\tau)\, \mathrm{d}\tau, \quad \Gamma_z(z) = \int_0^\infty \mathrm{e}^{-z\tau}\gamma_{zz}(\tau)\, \mathrm{d}\tau \quad (4.9)$$

with variable $z = -i\omega\tau_{Mx}$, and $z = -i\omega\tau_{Mz}$, respectively. It is convenient to use a common standard notation for the Laplace variable z.

In the limit $h \to \infty$, the reaction field factors tend to zero, and both functions in eq 4.9 tend to the simple expression

$$\Gamma_0(z) = \frac{1}{1 + \sigma\sqrt{z + z}} \quad (4.10)$$

with variable z defined as $z = -i\omega\tau_{M0}$ with relaxation time $\tau_{M0} = m^*/\zeta_0$ and with parameter σ given by

$$\sigma = \left(\frac{9m_f}{2m^*}\right)^{1/2} \quad (4.11)$$

as follows from the bulk admittance $\mathscr{Y}_0(\omega)$ given by eq 2.14. It is evident that the function $\Gamma_0(z)$ has a square root branch cut along the negative real axis. The term linear in $\sqrt{z}$ in the expansion about $z = 0$ is responsible for the $\tau^{-3/2}$ long-time tail in the relaxation function $\gamma_0(\tau)$. The long-time behavior is given by

$$\gamma_0(\tau) \approx \frac{\sigma}{2\sqrt{\pi}}\tau^{-3/2} \text{ as } \tau \to \infty \quad (4.12)$$

The corresponding long-time behavior of the velocity correlation function is

$$C_0(t) \approx \frac{1}{12}k_B T\sqrt{\rho}(\pi\eta t)^{-3/2} \text{ as } t \to \infty \quad (4.13)$$

It is interesting to note that this is independent of the mass or size of the Brownian particle.

The presence of the wall changes this behavior dramatically. Expanding the admittance $\mathscr{Y}_{xx}(\omega)$ in powers of α, we obtain

$$\mathscr{Y}_{xx}(\omega) = \mu_0[A_{x0} + A_{x2}(\alpha a)^2 + A_{x3}(\alpha a)^3] + O((\alpha a)^4) \quad (4.14)$$

with coefficients

$$A_{x0} = 1 - \frac{9a}{16h}$$

$$A_{x2} = -\frac{9h}{8a} + \frac{8}{9} - \frac{2m_p}{9m_f} - \frac{1}{8}\left(1 - \frac{m_p}{m_f}\right)\frac{a}{h}$$

$$A_{x2} = \frac{h^2}{a^2} - \frac{5}{9} + \frac{2m_p}{9m_f} + \frac{1}{8}\left(1 - \frac{m_p}{m_f}\right)\frac{a}{h} \quad (4.15)$$

Similarly, expanding the admittance $\mathscr{Y}_{zz}(\omega)$ in powers of α, we obtain

$$\mathscr{Y}_{zz}(\omega) = \mu_0[A_{z0} + A_{z2}(\alpha a)^2 + A_{z3}(\alpha a)^3] + O((\alpha a)^4) \quad (4.16)$$

with coefficients

$$A_{z0} = 1 - \frac{9a}{8h}$$

$$A_{z2} = -\frac{3h}{8a} + \frac{8}{9} - \frac{2m_p}{9m_f} - \frac{1}{4}\left(1 - \frac{m_p}{m_f}\right)\frac{a}{h}$$

$$A_{z3} = -\frac{5}{9} + \frac{2m_p}{9m_f} + \frac{1}{4}\left(1 - \frac{m_p}{m_f}\right)\frac{a}{h} \quad (4.17)$$

In both expansions, the term linear in αa is absent. The cancellation comes about on account of the values of the first two coefficients in the expansions (3.11) and (3.12). Such a term in the bulk admittance $\mathscr{Y}_0(\omega)$ is precisely the one responsible for the long-time tail in eq 4.13. The terms proportional to $(\alpha a)^3$ in eqs 4.14 and 4.16 imply that the functions $C_{xx}(t)$ and $C_{zz}(t)$ decay with a long-time tail proportional to $t^{-5/2}$. The coefficient of this long-time tail depends on the mass and size of the particle and on the distance to the wall. We can write the correlation functions in the form

$$C_{xx}(t) = C_0(t) + C_{1xx}(t), \quad C_{zz}(t) = C_0(t) + C_{1zz}(t) \quad (4.18)$$

Here the functions $C_{1xx}(t)$ and $C_{1zz}(t)$ describe the effect of the wall. These functions have a long-time tail as in eq 4.13 but with the opposite sign.

The above results suggest that the wall has a strong effect on the velocity autocorrelation function of a Brownian particle. In any case, the long-time tail is obliterated and replaced by a different long-time behavior. An investigation of the correlation functions over the whole range of time requires a study of the frequency-dependence of the admittance. The exact results given by eqs 2.13, 3.9, and 3.10 are quite complicated. The inverse Fourier transform of eq 4.2, with eq 4.3 substituted, cannot be obtained in explicit form. However, we can get an accurate numerical picture of the behavior in time of the correlation functions $C_{xx}(t)$ and $C_{zz}(t)$.

From the explicit expressions, it follows that the Laplace transform of the relaxation function has a Stieltjes representation of the form[17]

$$\Gamma(z) = \int_0^\infty \frac{p(u)}{u+z}\,\mathrm{d}u \quad (4.19)$$

The spectral density $p(u)$ can be found as

$$p(u) = -\frac{1}{\pi}\mathscr{I}\,\Gamma(z = -u + i0) \quad (4.20)$$

The spectral density has been normalized such that

$$\int_0^\infty p(u)\,\mathrm{d}u = 1 \qquad \int_0^\infty \frac{p(u)}{u}\,\mathrm{d}u = 1 \quad (4.21)$$

The inverse Laplace transform shows that the relaxation function $\gamma(\tau)$ is given by a superposition of purely decaying exponentials

$$\gamma(\tau) = \int_0^\infty p(u)\,e^{-u\tau}\,\mathrm{d}u \quad (4.22)$$

In the absence of the wall the Laplace transform of the relaxation function takes the form given in eq 4.10. The corresponding spectral density $p_0(u)$ reads

$$p_0(u) = \frac{1}{\pi}\frac{\sigma\sqrt{u}}{1 + (\sigma^2 - 2)u + u^2} \quad (4.23)$$

The relaxation function is given by

$$\gamma_0(\tau) = A_+ w(-iy_+\sqrt{\tau}) + A_- w(-iy_-\sqrt{\tau}) \quad (4.24)$$

where $w(z)$ is related to the error function of complex argument.[18] The coefficients $A_\pm$ are given by

$$A_\pm = \frac{\pm y_\pm}{\sqrt{\sigma^2 - 4}} \quad (4.25)$$

and the values $y_\pm$ by

$$y_\pm = -\frac{1}{2}\sigma \pm \frac{1}{2}\sqrt{\sigma^2 - 4} \quad (4.26)$$

The relaxation function has the long-time behavior

$$\gamma_0(\tau) \approx \frac{\sigma}{2\sqrt{\pi}}\tau^{-3/2} \text{ as } \tau \to \infty \tag{4.27}$$

We recall that for relaxation in the bulk the mean relaxation time is given by $\tau_{M0} = m^*/\zeta_0$. Correspondingly the effective mass m^* cancels in the long-time behavior, given by eq 4.13.

5. Effect of the Wall

The effect of a plane wall on the motion of a sphere in a viscous fluid was studied earlier by Wakiya[7] and by Gotoh and Kaneda.[8] Wakiya prescribed constant velocity starting suddenly from rest and calculated the corresponding time-dependent drag. Gotoh and Kaneda calculated the long-time tails of the velocity autocorrelation functions but did not take proper account of the particle equation of motion. Pagonabarraga et al.[9] provided a qualitative explanation of the long-time tails and presented computer simulation results for the velocity autocorrelation functions in the whole time regime.

One can see the relation to the work of Wakiya[7] and Gotoh and Kaneda[8] most readily by noting that in effect these authors calculated the reaction field factors. In the notation of Gotoh and Kaneda, the relation reads

$$F_{xx}(\boldsymbol{r}_0,\omega) = \frac{-\alpha}{8\pi\eta}(a_{\|} + b_{\|})$$
$$F_{zz}(\boldsymbol{r}_0,\omega) = \frac{-\alpha}{8\pi\eta}(a_{\perp} + b_{\perp}) \tag{5.1}$$

The quantities $a_{\|}$ and $b_{\|}$ were calculated as one-dimensional integrals by Wakiya.[1] His expression for $b_{\|}$ is quoted incorrectly by Gotoh and Kaneda;[8] there is a factor of 2 missing in the integrand in their eq 38b. The quantities $a_{\perp}$ and $b_{\perp}$ were calculated by Gotoh and Kaneda.[8] The identities eq 5.1 can be verified by use of eq 3.8 and our expressions 3.4−3.7 for the Green functions. A comparison of eqs 3.11 and 3.12 with eqs 40a and 40b of Gotoh and Kaneda shows that a term is missing in their eq 40a.

The expansion eq 4.14 leads to the long-time behavior

$$C_{xx}(t) \approx k_B T \frac{A_{x3}a^2}{\eta}\left(\frac{\rho}{4\pi\eta}\right)^{3/2} t^{-5/2} \text{ as } t \to \infty \tag{5.2}$$

In the corresponding expression of Gotoh and Kaneda the factor A_{x3} is replaced by h^2/a^2. For $h \gg a$ this is a good approximation, as follows from eq 4.15. To compare with their expression for the long-time tail of the function $C_{zz}(t)$ we must extend the expansion in eq 4.16 to order α^5. The corresponding coefficient A_{z5} is given by

$$A_{z5} = -\frac{1}{10}\frac{h^4}{a^4} - \frac{m_p - m_f}{m_f}\left(\frac{1}{12}\frac{h}{a} + \frac{8}{81}\frac{m_p - 4m_f}{m_f} - \frac{1}{36}\frac{4m_p - 7m_f}{m_f}\frac{a}{h}\right) \tag{5.3}$$

The expansion eq 4.16 leads to the long-time behavior

$$C_{zz}(t) \approx k_B T\left[\frac{A_{z3}a^2}{\eta}\left(\frac{\rho}{4\pi\eta}\right)^{3/2} t^{-5/2} - \frac{5A_{z5}a^4\rho}{2\eta^2}\left(\frac{\rho}{4\pi\eta}\right)^{3/2} t^{-7/2}\right] \text{ as } t \to \infty \tag{5.4}$$

In the corresponding expression of Gotoh and Kaneda the term with A_{z3} is missing, and the factor A_{z5} is replaced by $-h^4/10a^4$. For $h \gg a$ the second term in eq 5.4 may be larger than the first over a range of time, but eventually the first term dominates. Note that A_{z3} is negative for $(8h - 9a)m_p < (20h - 9a)m_f$, and that the second term is positive for sufficiently large ratio h/a.

Next we compare with the computer simulation results of Pagonabarraga et al.[9] These authors have studied velocity relaxation of a particle suspended in a fluid described by the lattice-Boltzmann model. In the model the fluid is compressible. The particle is assumed to be neutraly buoyant, i.e., $m_p = m_f$. We note that for a neutraly buoyant sphere the frequency-dependent admittance, given by eq 2.14, simplifies to

$$\mathscr{Y}(\boldsymbol{r}_0,\omega) = \mathscr{Y}_0(\omega)\mathbf{1} + \mathbf{F}(\boldsymbol{r}_0,\omega) \tag{5.5}$$

so that the difference of the velocity relaxation function from its bulk value is a direct measure of the reaction field tensor. Since the right-hand side of eq 5.5 is a sum, the $t^{-5/2}$ long-time tail in eq 5.2 is a linear combination of terms originating from the bulk admittance $\mathscr{Y}_0(\omega)$ and the reaction field factor $F_{xx}(\boldsymbol{r}_0,\omega)$. The first term in eq 5.4 originates exclusively from the bulk admittance, and the second term originates exclusively from the reaction field factor $F_{zz}(\boldsymbol{r}_0,\omega)$. For the neutraly buoyant case the functions $C_{1xx}(t)$ and $C_{1zz}(t)$ in eq 4.18 are simply k_BT times the inverse Fourier transform of the field factors $F_{xx}(\boldsymbol{r}_0,\omega)$ and $F_{zz}(\boldsymbol{r}_0,\omega)$.

We write the field factors, given by eqs 3.9 and 3.10, in the abbreviated form

$$F_{xx}(\boldsymbol{r}_0,\omega) = \frac{1}{6\pi\eta h}\phi_x(v), \quad F_{zz}(\boldsymbol{r}_0,\omega) = \frac{1}{6\pi\eta h}\phi_z(v) \tag{5.6}$$

with the variable $v = (-i\omega\rho/\eta)^{1/2}h$ as before. The functions $\phi_x(v)$ and $\phi_z(v)$ have Stieltjes representations in the complex frequency frame, as in eq 4.19, but with spectral densities that are not positive definite. We write the Stieljes representations in the form

$$\phi_x(v) = \int_0^\infty \frac{f_x(u)}{u + v^2}\,\mathrm{d}u, \quad \phi_z(v) = \int_0^\infty \frac{f_z(u)}{u + v^2}\,\mathrm{d}u \tag{5.7}$$

The spectral densities $f_x(u)$ and $f_z(u)$ can be found as

$$f_x(u) = -\frac{1}{\pi}\mathscr{I}\phi_x(v = i\sqrt{u}), \quad f_z(u) = -\frac{1}{\pi}\mathscr{I}\phi_z(v = i\sqrt{u}) \tag{5.8}$$

For large values of u the explicit expressions in eqs 3.9 and 3.10 lead to numerical difficulties. One can resolve these by using eq 3.8 directly to derive integral representations in terms of rapidly convergent contour integrals in the plane of complex wavenumber. At high u the spectral densities $f_x(u)$ and $f_z(u)$ oscillate about zero. In Figure 1, we plot the spectral density $f_x(u)$ as a function of log (u). In Figure 2, we present a similar plot for the function $f_z(u)$. The corresponding relaxation functions

$$\psi_x(\tau) = \int_0^\infty f_x(u)\mathrm{e}^{-u\tau}\,\mathrm{d}u, \quad \psi_z(\tau) = \int_0^\infty f_z(u)\,\mathrm{e}^{-u\tau}\,\mathrm{d}u \tag{5.9}$$

can be evaluated as functions of τ by numerical integration.

The complicated oscillatory behavior of the spectral densities for large u is relevant only for small values of τ. A good approximation for intermediate and large τ is obtained by approximating the spectral densities with the aid of Padé approximants.[17] From eq 4.4, one finds that for large positive

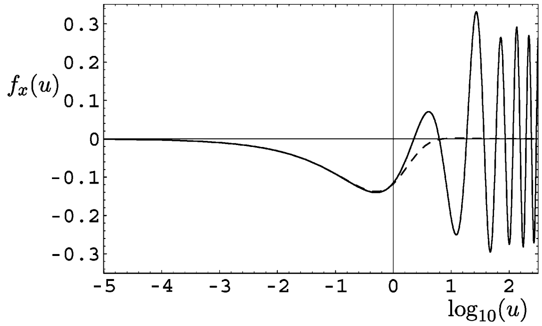

Figure 1. Plot of the spectral density $f_x(u)$ (solid curve) and the approximate spectral density $f_{xa}(u)$ (dashed curve) as functions of log (u).

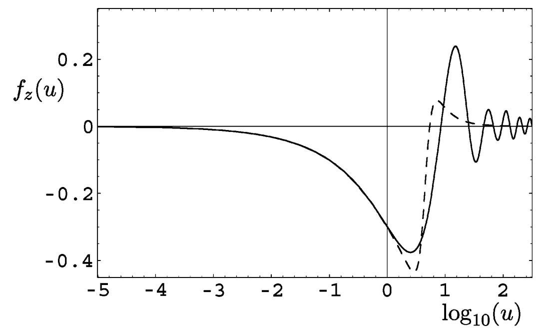

Figure 2. Plot of the spectral density $f_z(u)$ (solid curve) and the approximate spectral density $f_{za}(u)$ (dashed curve) as functions of log (u).

v the functions $\phi_x(v)$ and $\phi_z(v)$ behave as

$$\phi_x(v) \approx -\frac{3}{16v^2}, \quad \phi_z(v) \approx -\frac{3}{8v^2} \tag{5.10}$$

This corresponds to the initial values

$$\psi_x(0) = -\frac{3}{16}, \quad \psi_z(0) = -\frac{3}{8} \tag{5.11}$$

Combining eq 5.10 with the expansions for small v, given by eqs 3.11 and 3.12, we approximate $\phi_x(v)$ by

$$\phi_{xa}(v) = -\frac{3}{16}\frac{1341 + 208v}{447 + 864v + 642v^2 + 208v^3} \tag{5.12}$$

This reproduces the first four terms in the expansion eq 3.11 exactly. The corresponding approximate spectral density $f_{xa}(u)$ is shown also in Figure 1. Similarly the function $\phi_z(v)$ is approximated by

$$\phi_{za}(v) = -\frac{3}{8}\frac{608400 + 260992v + 19215v^2}{202800 + 267264v + 176373v^2 + 67688v^3 + 19215v^4} \tag{5.13}$$

This reproduces the first six terms in the expansion eq 3.12 exactly. The corresponding approximate spectral density $f_{za}(u)$ is shown also in Figure 2.

The approximate relaxation functions corresponding to the approximants $\phi_{xa}(v)$ and $\phi_{za}(v)$ can now be found by decomposition into sums of simple poles. Correspondingly, we find

$$\psi_{xa}(\tau) = \sum_{j=1}^{3} R_{xj} v_{xj} w(-i v_{xj}\sqrt{\tau}) \tag{5.14}$$

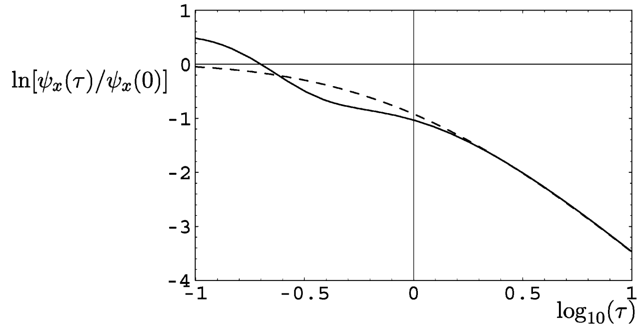

Figure 3. Plot of $\ln[\psi_x(\tau)/\psi_x(0)]$ (solid curve) and the approximant $\ln[\psi_{xa}(\tau))/\psi_x(0)]$ (dashed curve) as functions of log (τ).

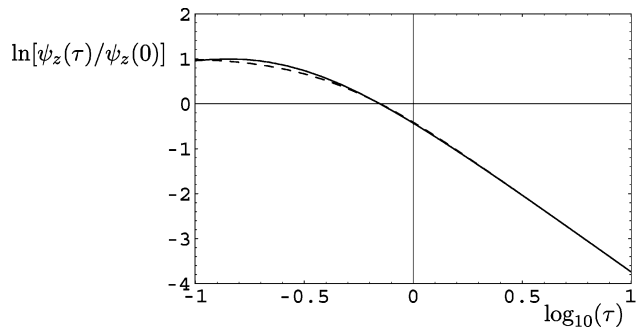

Figure 4. Plot of $\ln[\psi_z(\tau)/\psi_z(0)]$ (solid curve) and the approximant $\ln[\psi_{za}(\tau)/\psi_z(0)]$ (dashed curve) as functions of log (τ).

From eq 5.12, we find the values

$$R_{x1} = -1.019, \quad v_{x1} = -1.083$$
$$R_{x2,3} = 0.509 \pm 0.137\, i, \quad v_{x2,3} = -1.002 \pm 0.990\, i \tag{5.15}$$

Similarly we find for the relaxation function $\psi_{za}(\tau)$

$$\psi_{za}(\tau) = \sum_{j=1}^{4} R_{zj} v_{zj} w(-i v_{zj}\sqrt{\tau}) \tag{5.16}$$

From eq 5.13 we find the values

$$R_{z1,2} = 0.649 \pm 0.136\, i, \quad v_{z1,2} = -0.444 \pm 2.071\, i$$
$$R_{z3,4} = -0.649 \pm 0.601\, i, \quad v_{z3,4} = -1.317 \pm 0.786\, i \tag{5.17}$$

The approximate relaxation functions $\psi_{xa}(\tau)$ and $\psi_{za}(\tau)$ reproduce the initial values eq 5.11 and the long-time behavior exactly. In Figure 3, we show the exact function $\ln[\psi_x(\tau)/\psi_x(0)]$ as a function of log (τ), and compare with the approximate $\ln[\psi_{xa}(\tau)/\psi_x(0)]$. In Figure 4 we show the exact function $\ln[\psi_z(\tau)/\psi_z(0)]$ as a function of log (τ), and compare with the approximate $\ln[\psi_{za}(\tau)/\psi_z(0)]$. It is evident that at short times the exact functions oscillate about the approximate ones. The functions are not completely monotone, since the spectral densities $f_x(u)/\psi_x(0)$ and $f_z(u)/\psi_z(0)$, as well as the approximate $f_{xa}(u)/\psi_x(0)$ and $f_{za}(u)/\psi_z(0)$, are not positive definite.

For a neutraly buoyant particle, the complete relaxation functions are now given by

$$C_{xx}(t) = k_B T\left[\frac{1}{m^*}\gamma_0(t/\tau_{M0}) + \frac{1}{6\pi\rho h^3}\psi_x(t/\tau_w)\right]$$
$$C_{zz}(t) = k_B T\left[\frac{1}{m^*}\gamma_0(t/\tau_{M0}) + \frac{1}{6\pi\rho h^3}\psi_z(t/\tau_w)\right] \tag{5.18}$$

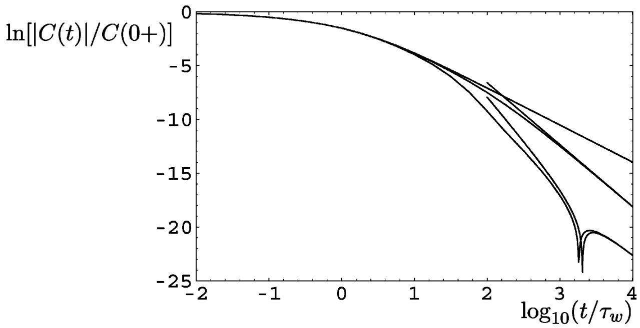

FIG. 5:

Figure 5. Plot of the functions $\ln[C_0(t)/C_0(0+)]$ (top curve), $\ln[C_{xx}(t)/C_{xx}(0+)]$ (middle curve), and $\ln[|C_{zz}(t)|/C_{zz}(0+)]$ (bottom curve) for a particle of radius $a = 0.5$ at a distance $h = 2.5$ from the wall in a fluid of mass density $\rho = 24$ and shear viscosity $\eta = 14.4$. The asymptotic curves, given by eq 5.20 are also drawn.

with characteristic time $\tau_w = \rho h^2/\eta$. It follows from eqs 3.11 and 3.12 that the functions $\psi_x(\tau)$ and $\psi_z(\tau)$ decay as

$$\psi_x(\tau) \approx -\frac{1}{2\sqrt{\pi}}\tau^{-3/2}, \quad \psi_z(\tau) \approx -\frac{1}{2\sqrt{\pi}}\tau^{-3/2} \text{ as } \tau \to \infty \quad (5.19)$$

Hence the long-time $t^{-3/2}$ tails cancel precisely, and one is left with the long-time behavior given by eqs 5.2 and 5.4 with

$$C_{xx}(t) \approx k_B T \frac{3h^2 - a^2}{3\eta}\left(\frac{\rho}{4\pi\eta}\right)^{3/2} t^{-5/2}$$

$$C_{zz}(t) \approx k_B T\left[-\frac{a^2}{3\eta}\left(\frac{\rho}{4\pi\eta}\right)^{3/2} t^{-5/2} + \frac{h^4\rho}{4\eta^2}\left(\frac{\rho}{4\pi\eta}\right)^{3/2} t^{-7/2}\right] \text{ as } t \to \infty \quad (5.20)$$

where we have used the expressions 4.15, 4.17, and 5.3 for a neutraly buoyant particle.

In Figure 5, we plot the reduced relaxation function $\ln[C_{xx}(t)/C_{xx}(0+)]$ as a function of $\log(t/\tau_w)$ for a neutraly buoyant particle of radius $a = 0.5$ at a distance $h = 2.5$ from the wall in a fluid of mass density $\rho = 24$ and shear viscosity $\eta = 14.4$. These values correspond to those in the computer simulation of Pagonabarraga et al.[9] We compare with the corresponding reduced function $\ln[C_0(t)/C_0(0+)]$ for relaxation in the bulk and with the long-time tail given by eq 5.20. We also plot the reduced relaxation function $\ln[|C_{zz}(t)|/C_{zz}(0+)]$ as a function of $\log(t/\tau_w)$. Again we compare with the long-time tail given by eq 5.20. In this case, the tail is negative at long times. In the computer simulation by Pagonabarraga et al.,[9] the fully asymptotic regime, where the tail becomes negative, was not reached (apparently they used $\log(t/\tau_w)$ along the abscissa of their Figure 6, rather than $\ln(t/\tau_w)$). At shorter times the authors see effects due to the finite velocity of sound.

For both $C_{xx}(t)$ and $C_{zz}(t)$, the relaxation function is well approximated for intermediate and large times by eq 5.18 together with eq 4.24 and eq 5.14 or 5.16. If the particle is not neutraly buoyant, one can use eq 2.13 together with eq 5.12 or 5.13 for the reaction field factor. The relaxation-functions are again well approximated by sums of w functions.

According to a general theorem about the analytic behavior of the admittance the spectral density corresponding to the trace $C_{xx}(t) + C_{yy}(t) + C_{zz}(t)$ is positive definite.[16] Hence, it follows that the sum of these velocity correlation functions is a completely monotone decreasing function of time.[19] The theorem does not hold for the individual terms. In fact, as we have shown above, $C_{zz}(t)$ has a negative long-time tail. The point approximation is not exact, so that the general theorem may be violated. It follows from eq 5.20 that the coefficient of the $t^{-5/2}$ tail of the trace is positive as long as $h^2 > a^2/2$.

6. Discussion

It has been shown that the Fourier transform of the velocity autocorrelation function of a Brownian particle near a wall in an incompressible viscous fluid can be obtained in explicit form. The wall has a profound effect on the long-time behavior. The nature of the long-time behavior reflects the macroscopic geometry. Even stronger effects can be expected for a particle located between two walls, or in cylindrical or spherical geometry.[20]

We note that the details of the time-dependence studied here have no consequences on the longer time scale of diffusion. Diffusion is affected by the presence of the wall only through its influence on the zero-frequency mobility, as given in point approximation by eqs 3.13 and 3.14, via the Einstein relation. The velocity correlation function decays on a faster time scale.

The suspending fluid has been assumed to be incompressible. Computer simulations have been performed for compressible fluids, both in single-wall,[9] two-wall,[21,22] and spherical geometry.[23] The velocity correlation functions that are found show a great deal of structure due to propagating or overdamped sound waves. It would be desirable to extend the theory developed here to these more complicated situations.

Acknowledgment. Dedicated in friendship to Professor I. Oppenheim.

References and Notes

(1) Zwanzig, R.; Bixon, M. *Phys. Rev. A* **1970**, *2*, 2005−2012.
(2) Widom, A. *Phys. Rev. A* **1971**, *3*, 1394−1396.
(3) Hauge, E. H.; Martin-Löf, A. *J. Stat. Phys.* **1973**, *7*, 259−281.
(4) Bedeaux, D.; Mazur, P. *Physica* **1974**, *76*, 247−258.
(5) Hinch, E. J. *J. Fluid Mech.* **1975**, *72*, 499−511.
(6) Lorentz, H. A. *Abh. Theor. Physik* **1907**, *1*, 23.
(7) Wakiya, S. *J. Phys. Soc. Jpn*. **1964**, *19*, 1401−1408.
(8) Gotoh, T.; Kaneda, Y. *J. Chem. Phys.* **1982**, *76*, 3193−3197.
(9) Pagonabarraga, I.; Hagen, M. H. J.; Lowe, C. P.; Frenkel, D. *Phys. Rev. E* **1998**, *58*, 7288−7295.
(10) Mazur, P.; Bedeaux, D. *Physica* **1974**, *76*, 235−246.
(11) Albano, A. M.; Bedeaux, D.; Mazur, P. *Physica A* **1975**, *80*, 89−97.
(12) Felderhof, B. U. *Physica A* **1976**, *84*, 569−576; **1976**, *88*, 614 (Erratum).
(13) Felderhof, B. U. *Physica A* **1990**, *166*, 492−504.
(14) Stokes, G. G. *Trans. Cambridge Philos. Soc.* **1851**, *9*, 8.
(15) Jones, R. B. *J. Chem. Phys.* **2004**, *121*, 483−500.
(16) Cichocki, B.; Felderhof, B. U. *Phys. Rev. E* **1995**, *51*, 5549−5555.
(17) Cichocki, B.; Felderhof, B. U. *Physica A* **1994**, *211*, 165−192.
(18) Abramowitz, M.; Stegun, I. A. *Handbook of Mathematical Functions*; Dover: Mineola, NY, 1965.
(19) Feller, W.; An Introduction to Probability Theory and Its Applications; Wiley: New York, 1971; Vol. II, p 439.
(20) Bocquet, L.; Barrat, J.-L. *J. Phys. Condens. Matter* **1996**, *8*, 9297−9300.
(21) Hagen, M. H. J.; Pagonabarraga, I.; Lowe, C. P.; Frenkel, D. *Phys. Rev. Lett.* **1997**, *78*, 3785−3788.
(22) Pagonabarraga, I.; Hagen, M. H. J.; Lowe, C. P.; Frenkel, D. *Phys. Rev. E* **1999**, *59*, 4458−4469.
(23) Bug, A. L. R.; Berne, B. J. *Phys. Rev. A* **1991**, *44*, 4953−4960.